

Support Vector Regression Machine Learning based Maximum Power Point Tracking for Solar Photovoltaic systems

Original Scientific Paper

P. Venkata Mahesh

Research Scholar, Department of Electronics and Instrumentation Engineering, Annamalai University, Chidambaram, Tamilnadu-608002, India. & Assistant Professor, Department of Electrical and Electronics Engineering, RVR & JC College of Engineering, Guntur, Andhra Pradesh-522019, India. vnktmahesh@gmail.com

S. Meyyappan

Assistant Professor, Department of Electronics and Instrumentation Engineering, Annamalai University, Chidambaram, Tamilnadu-608002, India. & Assistant Professor, Department of Instrumentation Engineering, Madras Institute of Technology, Chennai, Tamil Nadu-600044, India. meys.narayan@gmail.com

RamaKoteswaraRao Alla

Associate Professor, Department of Electrical and Electronics Engineering, RVR & JC College of Engineering, Guntur, Andhra Pradesh-522019, India. ramnitkkr@gmail.com

Abstract – Photovoltaic panels use the sun's radiation on their surface to convert solar energy into electricity. This process is dependent on the temperature of the surface and the intensity of the sun's radiation. To escalate the energy transformation, the solar system must be functioned at its maximum power point (MPP). Every maximum power point tracking (MPPT) technique has a distinct mechanism for tracking maximum power point (MPP). The support vector machine (SVM) regression algorithm is used in this work to develop a novel method for tracking the MPP of a PV panel. The solar panel technical parameters were used to prepare the data for training and testing the SVM model. The SVM algorithm predicts the PV panel's maximum power and relevant voltage for specific irradiation and temperature. The duty cycle of the boost converter corresponding to the maximum power was evaluated using the predicted values. The result of the simulation shows that the proposed control strategy forces the solar panel to work near the predicted MPP. The SVM regression control strategy gives the MPP tracking efficiency of more than 94% for the solar PV system despite variable climatic conditions during its stable state operation. In addition, a comparative analysis of the proposed method was carried out with the existing approaches to confirm the effective tracking of the proposed technique.

Keywords: Boost converter, MPPT, Photovoltaic system, Regression machine learning, Support vector machine

1. INTRODUCTION

The environmental harm produced by conventional power sources may be mitigated using solar energy. Photovoltaic generation systems (PVGS) convert solar energy into electricity. However, since the PVGS is not worked at maximum power point (MPP), it is strongly advised to drive the system at its MPP to enhance the energy conversion efficiency. This is achieved through a process known as maximum power point tracking (MPPT). The MPPT uses an algorithm to compel the PVGS to work at MPP. There are several MPPT approaches published in the literature. Each technique

has its own set of strengths and weaknesses and its own method of tracking the MPP. The conventional methods are the Perturb and Observe (P&O) [1] and incremental conductance (IC) [2] methods, mathematical methods such as curve fitting [3] and beta MPPT [4], measurement-based methods such as look-up table [5] and current sweep [6], constant parameter methods such as fractional open circuit voltage [7] and fractional short circuit current [8] methods, trial and error methods such as gradient descent method [9] and variable inductance method [10], optimization techniques like genetic algorithm [11], ant colony optimization [12], practical swarm optimization [13], gray wolf optimiza-

tion [14], and cuckoo search optimization [15], intellectual methods like an artificial neural network [16], fuzzy logic control [1], and ANFIS [1,9] are listed in the literature.

The need for clean, affordable, and sustainable energy is expanding rapidly, and technology is actively seeking methods to meet this need [17, 18]. The maximum power extraction from solar PV system is challenging task under partial shading conditions [19-21]. Artificial intelligence (AI) and machine learning (ML) have emerged as significant technological solutions. These cutting-edge technologies can forecast the future, enhance the present, and examine the past. This indicates that most of the current problems may be resolved using AI and ML [22]. Machine learning for MPPT typically eliminates the need for a controller. MPPT was implemented in the literature utilizing support vector machine learning in conjunction with a Proportional Integral Derivative (PID) controller [23], reinforcement learning [24], and a random forest technique [25]. The ML algorithm (MLA) may predict the unknown information if the model is trained, tested, and validated using existing information. Typically, the data for training, testing, and validating the machine learning model are chosen in the ratios of 60:20:20. Sum squared error (SSE), root mean square error (RMSE), and R^2 are three metrics that may use to assess the prepared model's prediction ability. For the calculation of RMSE, SSE, and R^2 , the following equations Eq. (1), (2), and (3) [26, 27] are used.

$$RMSE = \left[\frac{1}{n_s} \sum_{k=1}^{n_s} (Y_{A,k} - Y_{P,k})^2 \right]^{1/2} \quad (1)$$

$$SSE = \sum_{k=1}^{n_s} (Y_{A,k} - Y_{P,k})^2 \quad (2)$$

$$R^2 = 1 - \frac{\sum_{k=1}^{n_s} (Y_{A,k} - Y_{Avg})^2}{\sum_{k=1}^{n_s} (Y_{A,k} - Y_{Avg})^2} \quad (3)$$

where, Y_A is the real data, Y_P is the data predicted, the total samples number is n_s , and the real values average is Y_{Avg} . The R^2 is between 0 and 1 which gives the model prediction potential, and for the best suited model, the R^2 is near to 1. Similarly, the SSE and $RMSE$ quantifies the error among Y_P and Y_A . The model with the strongest ability to predict is therefore represented by $RMSE$ and SSE that are close to zero.

A power electronic converter is necessary to transmit the maximum amount of power from PVGS to the load. In literature, DC-DC converters such as the boost [2-6], buck-boost [7, 8], buck [10], and SEPIC [14] are employed. In addition, an inverter [9] can also be used to drive the ac loads or to supply the grid. This study proposes a unique method for tracking the MPP of a solar module using support vector machine regression learning. The suggested approach's efficacy was evaluated in contrast to classic MPPT algorithms such as P&O, IC methods, and intelligent control techniques such as ANN, FLC. The comparison has been done by considering time domain specifications of power response such as tracking speed, settling value, and overshoot, etc.

The rest of paper is organized as follows, the system description, which includes the PV module with technical parameters, boost converter, and support vector machine regression algorithm, is provided in Section-2; the methodology comprises collecting data, preparing the model, and PV panel working with support vector machine regression control approach have been provided in Section-3; simulation result with discussions of the proposed method are provided in Section-4, the proposed approach is compared with the existing P&O, IC, ANN and FLC methods in Section-5. The paper is concluded in Section-6.

2. DESCRIPTION OF SYSTEM

2.1. PV MODULE AND BOOST CONVERTER

Solar cells convert sunlight into electrical energy through photoelectric effect. Multiple solar cells connected to form a solar PV module. From the solar cell's single diode equivalent [28, 29] model the mathematical representation of solar module is in Eq.(4).

$$I_m = I_{PH} - I_0 \left(e^{\frac{V_m + I_m N_s R_s}{n N_s V_T}} - 1 \right) - \frac{V_m + I_m N_s R_s}{N_s R_{sh}} \quad (4)$$

where the solar module current is I_m and I_{PH} indicates the light generated current. The saturation current of the diode is I_0 , V is the module voltage, the ideal factor of pn-diode is n ($1 \leq n \leq 2$), the thermal voltage is V_T , and N_s is number of series cells. The resistances R_{sh} and R_s are the module shunt and series resistances respectively.

A 10W solar panel with 21.50V open circuit voltage, 0.62A short circuit current, 0.57A current and 17.50V voltage at MPP is used in this work. The current-voltage (I-V) and power-voltage (P-V) characteristics are provided in Fig.1.

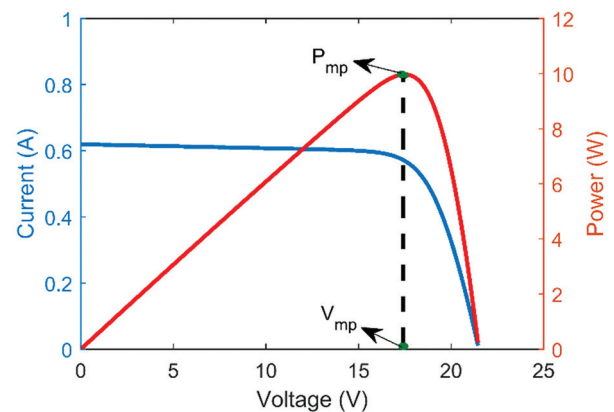


Fig. 1. I-V and P-V Characteristics of solar module at 1000w/m² and 25 °C

A dc-dc boost converter with pulse width modulation (PWM) control [29, 30] shown in Fig.2 is employed in this work. The power transferred to load from input source was controlled by using the duty cycle (D) of the switch. The inductor (L) enhances the input voltage to the necessary output value.

The input and output capacitors (C_i & C_o) both help to lower the voltage ripple content.

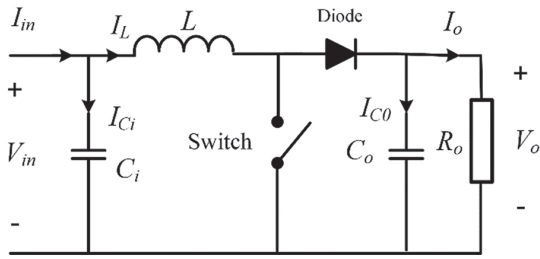


Fig. 2. DC-DC boost converter [29]

2.2. SUPPORT VECTOR MACHINE REGRESSION ALGORITHM

Support vector machines (SVM) were initially built to classify binary issues and were expanded to include the classification and regression of multiclass problems. In the training data set, by estimating the linear or nonlinear relationship between a given input and its associated output, the support vector machine regression (SVMR) technique [31] predicts the output based on the input. As a result, the developed SVMR model may be used to predict outcomes based on supplied inputs. The goal of support vector regression with ϵ -intense loss function is to determine the optimal hyperplane with the shortest distance between all data points. Suppose a training data set with N samples are denoted as $(x_i, y_i), i = 1, 2, \dots, N$, where x_i represents the input and y_i represents the output. The optimal hyperplane approximates the training points as closely as possible while reducing the prediction error. The linear hyperplane function is defined as $f(x) = \beta x + b$, where x denotes a point on the plane, β specifies the hyperplane's inclination in space, and b is the bias that determines the distance of the hyperplane from the origin, as shown in Fig. 3.

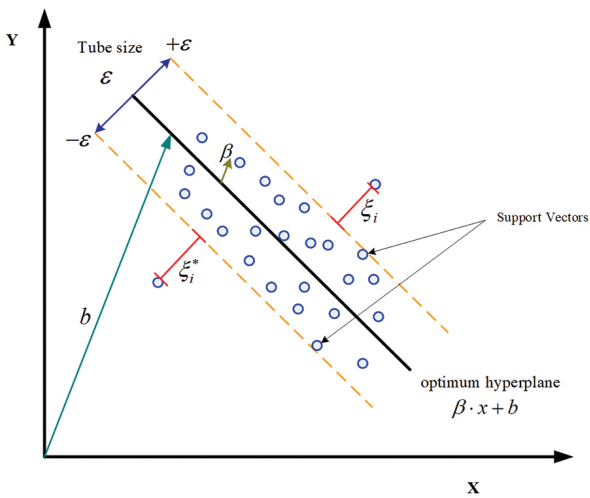


Fig. 3. SVM for linear regression problem on two dimensional space [31]

In the specified ϵ -insensitive loss function, SVMR looks for an ideal hyperplane that can predict y without errors.

In other terms, the distance between any data point and the ideal hyperplane is smaller than ϵ . Where ϵ represents the radius of the tube. SVMR uses a ϵ -intensive loss function to compute linear regression in a high-dimensional feature space while minimizing model complexity by reducing the value of $\|\beta\|^2$. The ϵ -intensive loss function is a function that is used to optimize generalization boundaries that are close to actual value and are located at a particular distance by ignoring errors. As a result, SVMR is defined as the solution to the optimization problem [31] given in Eq.(5) and Eq.(6).

$$\text{Minimize } \frac{1}{2} \|\beta\|^2 + C \sum_{i=1}^N (\xi_i - \xi_i^*) \quad (5)$$

$$\text{Subject to } \begin{cases} y_i - (\beta \cdot x_i + b) \leq \epsilon + \xi_i \\ (\beta \cdot x_i + b) - y_i \leq \epsilon + \xi_i^* \\ \xi_i \geq 0 \\ \xi_i^* \geq 0 \end{cases} \quad (6)$$

The slack variables ξ_i and ξ_i^* ($i = 1, 2, \dots, N$) will measure the deviation of the training samples outside the ϵ -insensitive zone, and the penalty parameter or the regularization constant is C which determines the trade-off between the model complexity and the training error. If the data has a non-linear shape, SVMR uses a non-linear transformation function ($K(x_i, x) = \phi(x_i) \cdot \phi(x)$) called a kernel function. This kernel is for mapping the input pattern to a high-dimensional feature space to identify the ideal hyperplane that minimizes discriminating errors in the training data. Next, a linear model is constructed in this feature space. As a result, the SVMR function for approximating nonlinear training data is as follows,

$$f(x) = \beta \times \phi(x) + b = \sum_{i=1}^N (\alpha_i - \alpha_i^*) K(x_i, x) + b \quad (7)$$

$$\beta = \sum_{i=1}^N (\alpha_i - \alpha_i^*) x_i \quad (8)$$

The kernel function in linear form is given by Eq.(9).

$$K(x_i, x) = x_i' \times x \quad (9)$$

The complementarity constraints by Karush Kuhn Tucker are optimization boundaries required to find the optimal solutions. These conditions are in Eq.(10) for Linear SVMR.

$$\left. \begin{aligned} \alpha_i (\epsilon + \xi_i - y_i + \beta \cdot x_i + b) &= 0 \\ \alpha_i^* (\epsilon + \xi_i^* + y_i - \beta \cdot x_i - b) &= 0 \\ \xi_i (C - \alpha_i) &= 0 \\ \xi_i^* (C - \alpha_i^*) &= 0 \end{aligned} \right\} \quad (10)$$

These circumstances address all perceptions rigorously inside the epsilon edge team having $\alpha_i = 0$ and $\alpha_i^* = 0$. An observation is called a support vector if either α_i or α_i^* is not zero. The difference between two support vectors Lagrange multipliers ($\alpha_i - \alpha_i^*$) is stored by the parameter a for a trained SVM model. The support vector's properties and bias store x_i and b , respectively. The type of kernel function and its parameters will decide the prediction performance of SVMR. The kernel functions are linear, radial basis, polynomial, and sigmoid [32]. Here, a linear kernel function is preferred as the data is almost linearly separable and is faster in training with fewer parameters to optimize.

3. METHODOLOGY

There are two phases in the proposed strategy. Obtaining data from the PV module specifications and creating the SVMR model comes in primary phase. The secondary is to employ the prepared SVMR model for MPPT. The power at MPP (P_{mp}) and the corresponding voltage at maximum power (V_{mp}) depends on irradiance (I_r) and temperature (T), so the T and I_r are used as input features in the prediction of P_{mp} and V_{mp} . The prepared SVMR models predict the P_{mp} and V_{mp} of the PV panel. The predicted P_{mp} and V_{mp} are used to compute the converter's duty cycle (D) such that the PV module works at the predicted MPP.

3.1. COLLECTING THE DATA & PREPARING THE MODEL

I_r , T , P_{mp} , and V_{mp} are the data needed for training and testing of the model. Solar panel parameters were used to gather the data. Matlab/Simulink software used to train the SVMR models. The flowchart in Fig. 4 depicts the process for gathering data and building a machine learning (ML) model.

3.2. SVMR MPPT CONTROL STRATEGY

For the input features I_r and T , the trained ML model predicts the P_{mp} and V_{mp} . The R_{mp} resistance, which corresponds to MPP, is evaluated using the predicted values P_{mp} and V_{mp} as in Eq.(11) [30]. In Fig. 5, R_{mp} will be replicated across node-p and node-q by controlling D of the boost converter. According to Figs. 4 and 7, the resistance (R_{pq}) between nodes p and q is zero when D is zero. As D grows, R_{pq} rises and will reach R_0 when D is one. The parameter D in R_{mp} and load resistance (R_0) is in Eq.(12) [30].

$$R_{mp} = \frac{V_{mp}^2}{P_{mp}} \quad (11)$$

$$D = 1 - \sqrt{\frac{R_{mp}}{R_0}} \quad (12)$$

The extreme and least values for load resistance are calculated using the method recommended by Razman Ayop et al. in [30]. The boost converter's design procedure is explained by Muhammad H. Rashid [33]. Equation (13) gives the boost converter inductance, and Eq.(14) provides the capacitance, respectively [33].

$$L = \frac{V_{ip} \times (V_{op} - V_{ip})}{f_{sw} \times \Delta I \times V_{op}} \quad (13)$$

$$C = \frac{I_{op} \times (V_{op} - V_{ip})}{f_{sw} \times \Delta V \times V_{op}} \quad (14)$$

where V_{ip} denotes input voltage, V_{op} denotes output voltage, f_{sw} indicates frequency of switching, ΔI represents current ripple, and ΔV represents voltage ripple. The control strategy diagram for the solar PV module with the SVM regression ML is shown in Fig. 5.

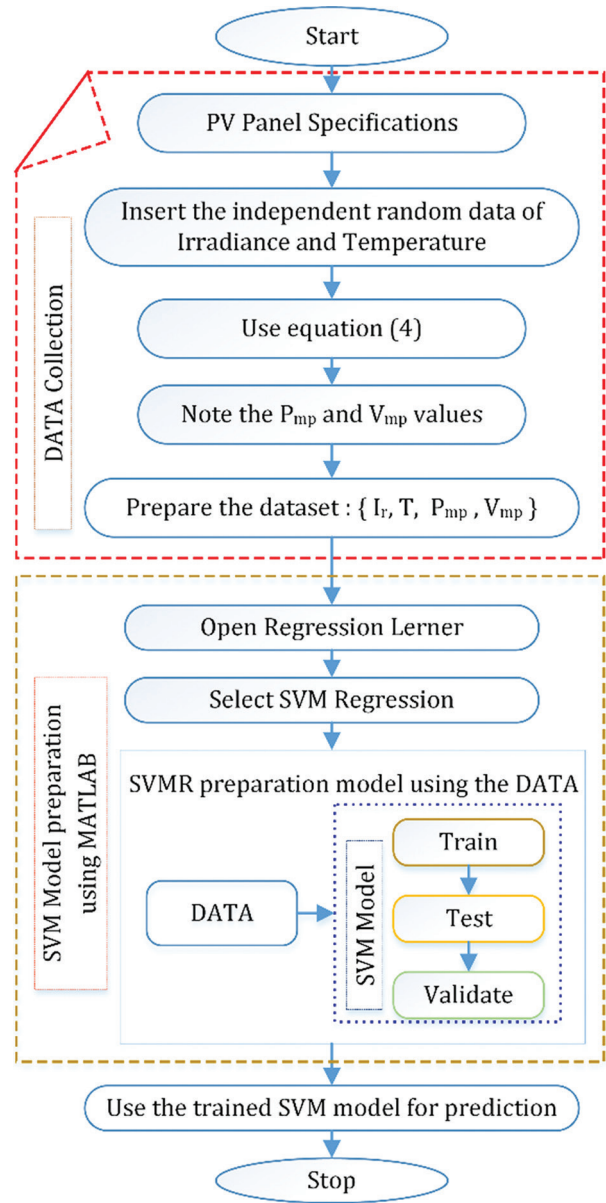


Fig. 4. Data collecting and ML model building procedure as a flowchart

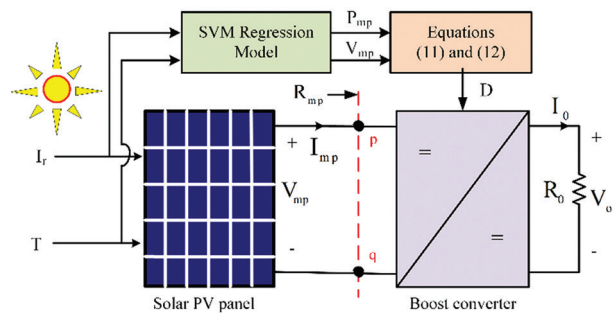


Fig. 5. Control strategy block diagram with SVM regression ML & dc-dc boost converter

4. SIMULATION RESULTS OF PROPOSED SVMR MPPT CONTROL STRATEGY

With the aid of solar panel technical parameters, the data from the PV panel has been collected in the sug-

gested method specified in section-3. The pairwise relation and correlation among the data is given in [29]. To test the tracking performance of the proposed technique in the presence of variables I_r and T , the simulation was run in four intervals of 0.5 seconds. For each interval either I_r or T are changed while keeping the other fixed. This variation is shown in Table -1.

Table 1. Input parameters of the PV panel for various intervals

Parameter	Interval-1	Interval-2	Interval-3	Interval-4
Time (sec)	0 to 0.5	0.5 to 1	1 to 1.5	1.5 to 2
I_r (W/m ²)	450	450	950	950
T (°C)	25	35	35	25

The simulation values used here in study are, PV power (P) = 10W, f_{sw} = 5 kHz, ripple voltage allowed (ΔV) = 1 %, ripple current allowed (ΔI) = 5 %, L = 34 mH, C_o = 68 μ F, R_o = 300 Ω , and C_i = 1000 μ F.

Table 2. Parameters of created the SVMR models with linear kernel

Parameter	SVMR-1 (P_{mp} plane)	SVMR-2 (V_{mp} plane)
Bias	0.4568	19.1963
ϵ	0.4224	0.0397
β	[0.0091 -9.4161 $\times 10^{-4}$]	[4.2608 $\times 10^{-4}$ -0.0802]
No. of support vectors	3	30
No. of iterations	9	1 $\times 10^6$

The SVMR models (SVMR-1 and SVMR-2) are created with I_r and T input features. The output predicted response for SVMR-1 is P_{mp} and for SVMR-2 is V_{mp} . The parameters of the created models are in Table-2. The actual and predicted data by the developed SVMR models are given in Fig. 6. Fig. 6a shows a small residual in prediction on the P_{mp} plane. On the other side Fig. 6b shows that for low I_r and T , the prediction error is high, and for the rest is minor on the V_{mp} plane.

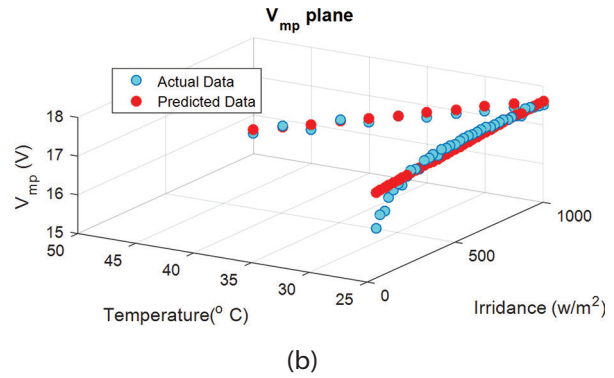
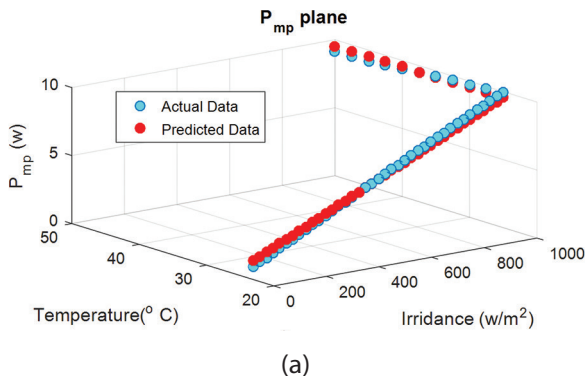


Fig. 6. Predicted and actual data by a) SVMR-1 on P_{mp} plane b) SVMR-2 on V_{mp} plane

Fig. 7 indicates the solar panel and load V , I , and power (P) responses with the developed SVMR models. These results illustrate a small oscillation in the transient response if there is a variation in T and fluctuations with large amplitude if I_r is varied. Figure 8 shows the tracking efficiency and comparison of the predicted and working PV power. It can be observed that the proposed methodology tracks the accurate MPP in the stable state.

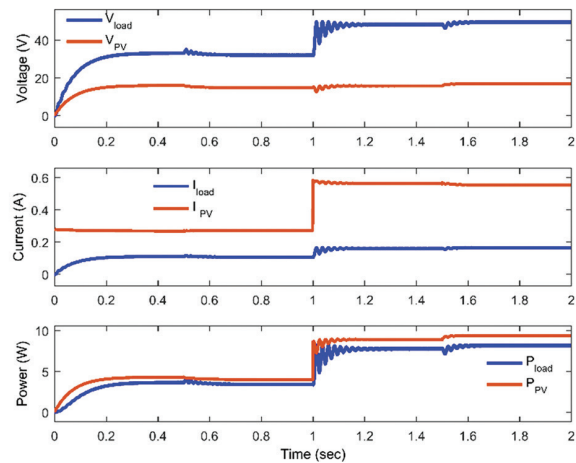


Fig. 7. The load and solar panel V , I and P responses with SVMR models

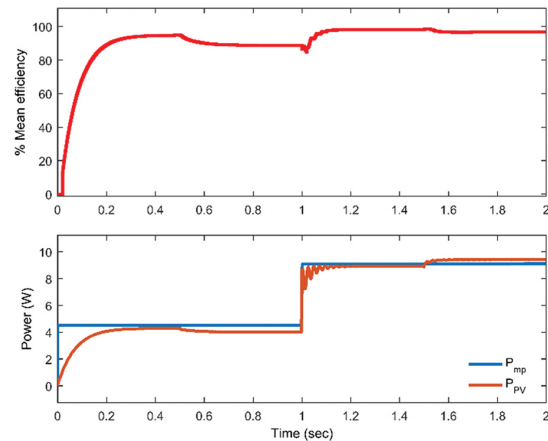


Fig. 8. Mean efficiency (%), P_{mp} and P_{pv} waveforms with SVMR models

5. PERFORMANCE COMPARISON PROPOSED METHOD WITH EXISTING METHODS

In this section, the results of the proposed control strategy are compared with the classical methods like perturb and observe (P&O) and incremental conductance (IC) and intelligent methods like artificial neural network (ANN) and fuzzy logic control (FLC).

5.1. WITH P&O METHOD

The P&O algorithm [1] controls the duty cycle (D) of the converter depending on the PV panel's present voltage and power values. The predicted maximum power P_{mp} by the SVMR model, proposed SVMR strategy (P_{svmr}), and P&O method responses are compared in Fig. 9. The $P_{p\&o}$ response has continuous oscillations near the MPP. In contrast, the proposed SVMR methodology response is not having any oscillations in the steady state. Therefore, the SVMR method operates the solar panel almost nearer to MPP, even in variable I_r and T presence.

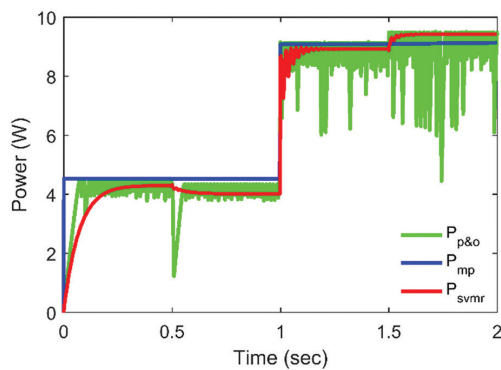


Fig. 9. Comparative plot for P_{mp} , P_{svmr} and $P_{p\&o}$

5.2. WITH IC METHOD

The IC method [2] controls the converter's D depending on the voltage and current values of the PV panel. The predicted P_{mp} by the SVMR model, IC algorithm (P_{ic}), and proposed SVMR strategy (P_{svmr}) responses are compared in Fig. 10. The P_{ic} response has continuous oscillations near the MPP. On the other hand, the proposed SVMR methodology operates the solar panel nearer to MPP with no fluctuations under variable climatic conditions in the steady state.

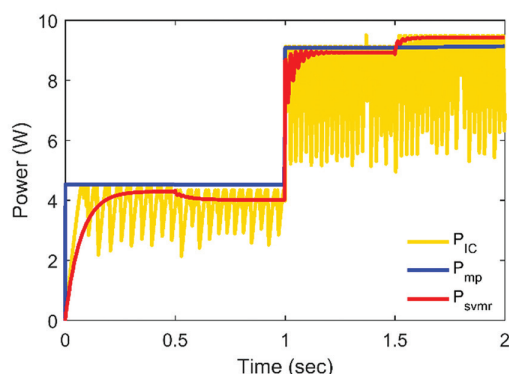


Fig. 10. Comparative plot for P_{mp} , P_{svmr} and P_{ic}

5.3. WITH ANN METHOD

The proposed control strategy results are compared with the perceptron type ANN MPPT [26, 29]. The ANN was trained with the same data used for SVMR model training. The ANN model's inputs are I_r , T , and outputs are P_{mp} , V_{mp} . Ten hidden layer and two output layer neurons make up the ANN architecture [29]. The data were decomposed to training data, validating data, and testing data for the ANN model in 60%, 20%, and 20%, respectively.

In Fig. 5, the SVMR ML model is replaced with the trained ANN model for MPPT. The P_{mp} predicted by the SVMR model, ANN algorithm (P_{nn}), and proposed SVMR strategy (P_{svmr}) are compared in Fig. 11. The ANN algorithm works at MPP for low values of I_r . But if there is a huge change in the value of I_r , the ANN algorithm has large magnitude continuous oscillations, and for high values of I_r , the power response has small fluctuations near MPP in the steady state. The proposed SVMR approach provides the operation of the PV panel nearly at MPP with a small residual value under variable I_r and T in the steady state.

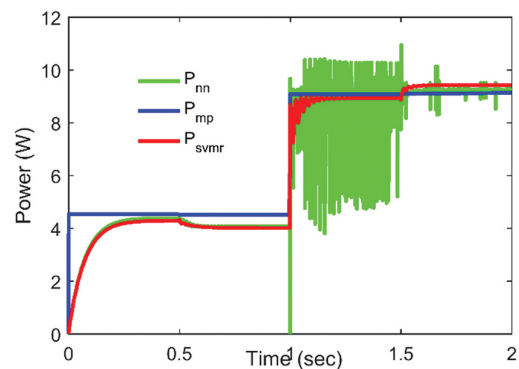


Fig. 11. Comparative plot for P_{mp} , P_{svmr} and P_{nn}

5.4. WITH FLC METHOD

Fuzzy logic control (FLC) [1, 27] handles the system's nonlinearities in a better way, no need a precise mathematical model and also works with defective inputs. The variation in D (ΔD) is FLC output. The duty ratio for the converter is determined by Eq.(18). Fig. 12 shows the triangular membership functions of FLC. The variables negative big & small (NB & NS), zero (ZE), and positive big & small (PB & PS) are allotted to membership functions with fuzzy subsets. Table-3 provides the rule base of FLC.

$$D(k+1)=D(k)+\Delta D \quad (18)$$

The predicted P_{mp} by the SVMR model, P_{svmr} and FLC method (P_{flc}), are compared in Fig. 13. The FLC response is similar to that of the SVMR method. But the FLC performance is based on the designed rule base, which needs humanoid experience and expertise. In Fig.13 (the portion in zoom) it is seen that if there is a huge increment in the I_r , there is a short duration overshoot with the FLC method. On the other hand, the SVMR method does not have it.

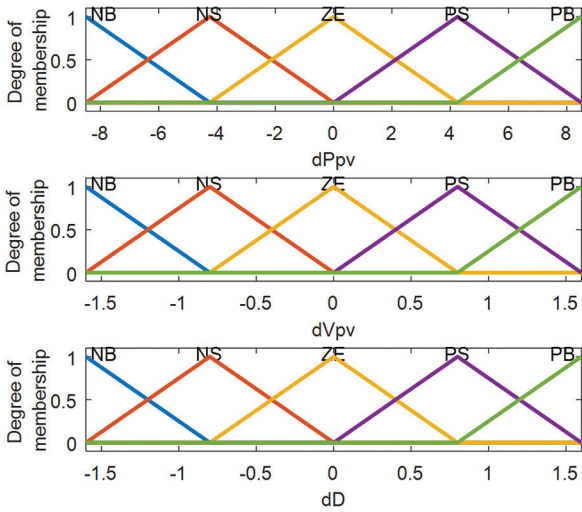


Fig. 12. ΔP_{pv} , ΔV_{pv} , and ΔD membership functions

Table 3. Fuzzy rule base

Output ΔD		Input-2 ΔV_{pv}				
		PB	PS	ZE	NS	NB
Input-1 ΔP_{pv}	NB	NS	NB	NB	PB	PS
	NS	NS	NS	NS	PS	PS
	ZE	ZE	ZE	ZE	ZE	ZE
	PS	PS	PS	PS	NS	NS
	PB	PB	PS	PS	NB	NS

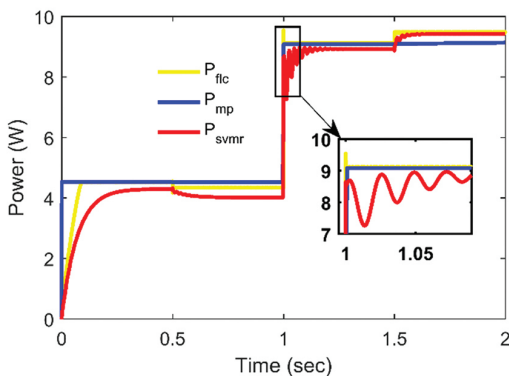


Fig. 13. Comparative plot for P_{mp} , P_{svmr} and P_{flc}

The predicted P_{mp} by the SVMR model, P_{svmr} and FLC method (P_{flc}), are compared in Fig. 13. The FLC response is similar to that of the SVMR method. But the FLC performance is based on the designed rule base, which needs humanoid experience and expertise. In Fig.13 (the portion in zoom) it is seen that if there is a huge increment in the I_r , there is a short duration overshoot with the FLC method. On the other hand, the SVMR method does not have it.

5.5. POWER RESPONSE COMPARISON DURING 0 TO 0.5 SEC (INTERVAL-1)

The SVMR model dynamic power response was compared with a few models in literature as a graphical in

Fig. 14 and numerically as time-domain values in Table-4 during the time interval-1. Fig. 14 demonstrates that, in the steady state, the IC and P&O techniques have oscillatory responses while the other methods do not exhibit them.

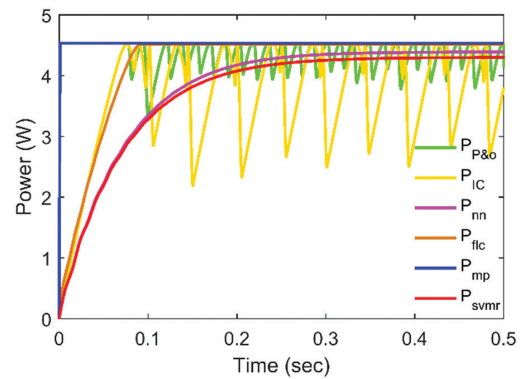


Fig. 14. PV power response comparison for various methods (interval-1)

Table-4 shows that, as compared to P&O, the proposed SVMR model response has settled approximately half as fast with a superior settling power of 3.8960 W and no overshoot. Compared to incremental conductance method, the SVMR model response has settled almost in half time with a better final value and with no overshoot. Regarding settling time, final value, and overshoot, the SVMR model response beats the P&O and IC techniques. The SVMR model power response numerical values are nearly similar to the intellectual method ANN. The FLC model power response is superior in numerical during 0 to 0.5 sec, but the FLC response depends on the strength of the rule base, which requires human experience and expertise. This comparative analysis shows that the proposed SVMR control strategy is good at chasing the MPP for PV systems under variable weather situations.

Table 4. MPP tracking response numerical comparison for various approaches

Parameter	SVMR	P & O	IC	ANN	FLC
Rise Time (sec)	0.1558	0.0519	0.0470	0.1541	0.0690
Peak Time (sec)	0.5	0.4989	0.1327	0.5	0.5
Peak value (W)	4.3288	4.5211	4.5211	4.4195	4.5512
Settling Min. (W)	3.8960	3.3161	2.1899	3.9777	4.1186
Settling Time (sec)	0.2846	0.5	0.4992	0.2762	0.0868
Undershoot (%)	0	0	0	0	0
Overshoot (%)	0	9.1727	18.8405	0	0

6. CONCLUSION

In this work, a new SVMR machine learning-based approach for MPPT of the solar panel is used in association with a PWM control boost converter. The mean efficiency value was determined to be greater than 94 per cent in steady state to confirm the efficacy of the SVMR algorithm. The SVMR approach has produced better MPPT outcomes than traditional perturb and observe and incremental conductance algorithms, intellectual prediction artificial neural network and fuzzy logic control algorithms, and even under dynamic climate. Furthermore, the simulation results demonstrate greater accuracy in tracking and working the system at MPP with the proposed SVMR control strategy in the steady state.

7. REFERENCES

- [1] A. S. Mahdi, K. Mahamad, S. Saon, T. Tuwoso, H. Elmunsyah, S. W. Mudjanarko, "Maximum power point tracking using perturb and observe, fuzzy logic and ANFIS", *SN Applied Sciences*, Vol. 2, No. 1, 2020, pp.1-9.
- [2] L. Shang, H. Guo, W. Zhu, "An improved MPPT control strategy based on incremental conductance algorithm", *Protection and Control of Modern Power Systems*, Vol. 5, No. 1, 2020, pp.1-8.
- [3] C. González-Castaño, L. L. Lorente-Leyva, J. Muñoz, C. Restrepo, D. H. Peluffo-Ordóñez, "An MPPT strategy based on a surface-based polynomial fitting for solar photovoltaic systems using real-time hardware", *Electronics*, Vol. 10, No. 2, 2021, 206.
- [4] X. Li, H. Wen, C. Zhao, "Improved beta parameter based MPPT method in photovoltaic system", *Proceedings of the 9th International Conference on Power Electronics and ECCE Asia*, Seoul, Korea, 1-5 June 2015, pp. 1405-1412.
- [5] V. R. Kota, M. N. Bhukya, "A simple and efficient MPPT scheme for PV module using 2-dimensional lookup table", *Proceedings of the IEEE Power and Energy Conference at Illinois, Urbana, IL, USA*, 19-20 February 2016, pp. 1-7.
- [6] M. Kaffash, M. H. Javidi, A. Darudi, "A combination maximum power point tracking algorithm in photovoltaic systems under partial shading conditions", *Proceedings of the Iranian Conference on Renewable Energy & Distributed Generation*, Mashhad, Iran, 2-3 April 2016, pp. 103-107.
- [7] D. Baimel, S. Tapuchi, Y. Levron, J. Belikov, "Improved fractional open circuit voltage MPPT methods for PV systems", *Electronics*, Vol. 8, No. 3, 2019, p. 321.
- [8] H. A. Sher, A. F. Murtaza, A. Noman, K. E. Ad-doweesh, K. Al-Haddad, M. Chiaberge, "A new sensorless hybrid MPPT algorithm based on fractional short-circuit current measurement and P&O MPPT", *IEEE Transactions on Sustainable Energy*, Vol. 6, No. 4, 2015, pp. 1426-1434.
- [9] K. Amara, T. Bakir, A. Malek, D. Hocine, E. B. Bourenane, A. Fekik, M. Zaouia, "An Optimized Steepest Gradient Based Maximum Power Point Tracking for PV Control Systems", *International Journal on Electrical Engineering & Informatics*, Vol. 11, No. 4, 2019, pp. 662-683.
- [10] L. Zhang, W. G. Hurley, W. H. Wölfle, "A new approach to achieve maximum power point tracking for PV system with a variable inductor", *IEEE Transactions on Power Electronics*, Vol. 26, No. 4, 2010, pp. 1031-1037.
- [11] S. Hadji, J. P. Gaubert, F. Krim, "Real-time genetic algorithms-based MPPT: study and comparison (theoretical and experimental) with conventional methods", *Energies*, Vol. 11, No. 2, 2018, p. 459.
- [12] G. S. Krishnan, S. Kinattungal, S. P. Simon, P. S. R. Nayak, "MPPT in PV systems using ant colony optimisation with dwindling population", *IET Renewable Power Generation*, Vol. 14, No. 7, 2020, pp. 1105-1112.
- [13] M. Alshareef, Z. Lin, M. Ma, W. Cao, "Accelerated particle swarm optimization for photovoltaic maximum power point tracking under partial shading conditions", *Energies*, Vol. 12, No. 4, 2019, 623.
- [14] K. Atici, I. Sefa, N. Altin, "Grey wolf optimization based MPPT algorithm for solar PV system with SEPIC converter", *Proceedings of the 4th International Conference on Power Electronics and their Applications*, Elazig, Turkey, 25-27 September 2019, pp. 1-6.
- [15] M. I. Mosaad, M. abed el-Raouf, M. A. Al-Ahmar, F. A. Banakher, "Maximum power point tracking of PV system based cuckoo search algorithm; review and comparison", *Energy Procedia*, Vol. 162, 2019, pp. 117-126.

- [16] L. P. N. Jyothy, M. R. Sindhu, "An Artificial Neural Network based MPPT Algorithm For Solar PV System", Proceedings of the 4th International Conference on Electrical Energy Systems, Chennai, India, 07-09 February, 2018, pp. 375-380.
- [17] N. Dharani Kumar, T. A. Ramesh Kumar, A.R.K. Rao, "A Brief Review on Conventional and Renewable Power Generation Scenario in India", Proceedings of the 2nd Electric Power and Renewable Energy Conference, Lecture Notes in Electrical Engineering, Vol. 812, February 2022.
- [18] S. Vunnam, M. Vanitha Sri, A.R.K. Rao, "Performance analysis of mono crystalline, poly crystalline and thin film material based 6×6 T-C-T PV array under different partial shading situations", Optik, Vol. 248, 2021, p.168055.
- [19] R. Kandipati, T. Ramesh, "Maximum power enhancement under partial shadings using a modified Sudoku reconfiguration", CSEE Journal of Power and Energy Systems, Vol. 7, No. 6, 2021, pp. 1187-1201.
- [20] T. Ramesh, K. Rajani, A. K. Panda, "A novel triple-tied-cross-linked PV array configuration with reduced number of cross-ties to extract maximum power under partial shading conditions", CSEE Journal of Power and Energy Systems, Vol. 7, No. 3, 2021, pp. 567-581.
- [21] K. Rajani, T. Ramesh, "Reconfiguration of PV arrays (TCT, BL, HC) by considering wiring resistance", CSEE Journal of Power and Energy Systems, Vol. 8, No. 5, 2022, pp. 1408-1416.
- [22] S. Chatterjee, R. Chaudhuri, S. Kamble, S. Gupta, U. Sivarajah, "Adoption of Artificial Intelligence and Cutting-Edge Technologies for Production System Sustainability: A Moderator-Mediation Analysis", Information Systems Frontiers, 2022, pp. 1-16.
- [23] M. Takruri et al. "Maximum power point tracking of PV system based on machine learning", Energies, Vol. 13, No. 3, 2020, p. 692.
- [24] Y. Chou, "Maximum Power Point Tracking of Photovoltaic System Based on Reinforcement Learning", Sensors, Vol. 19, No. 22, 2019, p. 5054.
- [25] H. Shareef, A. H. Mutlag, A. Mohamed, "Random Forest-Based Approach for Maximum Power Point Tracking of Photovoltaic Systems Operating under Actual Environmental Conditions", Computational Intelligence and Neuroscience, Vol. 2017, 2017, 17 pages.
- [26] K. Bingi, B. R. Prusty, "Chaotic time series prediction model for fractional-order duffing's oscillator", Proceedings of the 8th International Conference on Smart Computing and Communications, Kochi, Kerala, India, 1-3 July 2021, pp. 357-361.
- [27] P. V. Mahesh, S. Meyyappan, R. K. R. Alla, "A New Multivariate Linear Regression MPPT Algorithm for Solar PV System With Boost Converter", ECTI Transactions on Electrical Engineering, Electronics, and Communications, Vol. 20, No. 2, 2022, pp. 269-281.
- [28] V. Tamrakar, S. C. Gupta, Y. Sawle, "Single-diode PV cell modeling and study of characteristics of single and two-diode equivalent circuit", Electrical and Electronics Engineering: An International Journal, Vol. 4, No.3, 2015, p. 12.
- [29] P. V. Mahesh, S. Meyyappan, A. R. K. Rao, "Maximum Power Point Tracking with Regression Machine Learning Algorithms for Solar PV Systems", International Journal of Renewable Energy Research, Vol. 12, No. 3, 2022, pp. 1327-1338.
- [30] R. Ayop, C. W. Tan, "Design of boost converter based on maximum power point resistance for photovoltaic applications", Solar Energy, Vol. 160, 2018, pp. 322-335.
- [31] B. Ergun, T. Kavzoglu, I. Colkesen, C. Sahin, "Data filtering with support vector machines in geometric camera calibration", Optics express, Vol. 18, No.3, 2010, pp. 1927-1936.
- [32] H. Hong, B. Pradhan, D. T. Bui, C. Xu, A. M. Youssef, W. Chen, "Comparison of four kernel functions used in support vector machines for landslide susceptibility mapping: a case study at Suichuan area (China)", Geomatics, Natural Hazards and Risk, Vol. 8, No. 2, 2017, pp. 544-569.
- [33] M. H. Rashid, "Power electronics: circuits, devices, and applications", 4th Edition, Pearson Education India, 2009.